ICAS 2016
30th Congress of the International Council of the Aeronautical Sciences
DCC, Daejeon, Korea : September 25-30, 2016

SPECIAL CONSIDERATIONS TO THERMAL BEHAVIOR MODELING AND SIMULATION OF AN AEROSPACE ELECTROMECHANICAL ACTUATION SYSTEM

Jian Fu*,, Yongling Fu*, Jean-Charles Maré****
***Beihang University, Beijing 100191, China**
****Institut Clément Ader, INSA, Toulouse 31400, France**
fujianbuaa@126.com, fuyongling@126.com, jean-charles.mare@insa-toulouse.fr

Keywords: *Bond-graph, EMA, power-by-wire, power loss, thermal modeling*

Abstract

For the next generation of "more electric or all electric aircraft", there is a significant interest in using electromechanical actuators (EMAs) for flight controls, thrust reverse and landing gears, and therefore remove the centralized hydraulic circuits. To achieve this goal, new challenges for safety-critical actuations must be faced and several key issues must be considered in the early phases of the design process, such as jamming, thermal behavior, dynamics, etc. This communication deals with the analysis of EMA thermal behavior. The Bond-graph formalism is used to support the EMA thermal model architecting. On the basis of model based system engineering (MBSE), the effort is in architecting the models of energy losses to make them "ready for" extensive system-level simulation. Because of the multi-domain coupling, the EMA topology is decomposed into generic components and bodies, ensuring mechanically and energy balances. A simple and an advanced thermal models' architecture are developed to help analyzing the performance characteristics of the heat transfer in EMA. The models are causal and can be implemented in today's commercial simulation software to assess the EMA energy consumption and heat transfer.

1 Introduction

The aerospace industry is looking for the innovative technologies toward greener, safer and cheaper commercial air transports to bring the environmental, competitive and economic benefits. Many research activities have been engaged for the development of novel generation of aircrafts, such as the recent evolution towards "More Electric Aircraft" (MEA) and "All Electric Aircraft" (AEA). As far as possible, the conventional hydraulic, pneumatic and mechanical power networks are reduced or eliminated and progressively replaced by electrical ones [1]. Today, a number of challenges are introduced on the basis of the MEA and AEA concepts, the conventional in-service Fly-by-Wire (FbW) hydraulic servo actuators (HSAs) have been replaced by the becoming mature Power-by-Wire (PbW) actuators in some fields of more electrical actuation system, such as flight controls, landing gears and thrust reverser. Some PbW actuators are already in service the latest generation commercial aircrafts:

- Electro-hydrostatic actuators (EHAs) as backup actuators for primary and secondary flight controls in Airbus A380/A350,
- Electro-mechanical actuators (EMAs) as a few secondary flight controls and for braking in Boeing B787.

For PbW actuators, increased use of EMAs is becoming more and more attractive in aircraft system when compared to EHAs. Not only EMA is the ultimate form of AEA actuator, but also it has the potential benefits of aircraft fuel reduction, maintenance cost saving, and system flexibility improvement. However, the maturity of EMAs technology is still lagging. They suffer from some key issues, in particular such as huge reflected inertia, heat rejection, thermal and

mechanical balances, reaction forces to airframe, response to failure and etc. Thus, putting EMAs in front line of some safety-critical actuation system (like primary flight controls) is still not ready for extensive use in civil airplane applications. Another implementation of EMA has been tested for primary flight control in 2011 on an A320 as an aileron actuator [2].

In fact, one real challenge for the implementation of the EMA, serving in front line for primary flight controls or even non safety-critical actuation systems, comes from the thermal behavior that is addressed in this communication. According to Fig. 1, a linear EMA is electrically supplied and consists of a power drive electronics (PDE) that drives a rotary electric motor (EM) and a mechanical power transmission (MPT), which involves a nut-screw (NS), and an intermediate gearbox when necessary.

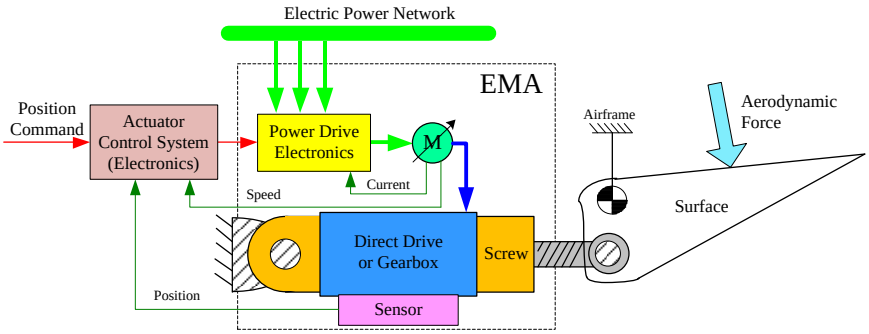

Fig. 1. Schematic of an EMA Flight Control Actuation System

The thermal behavior in such compact system is not easy to address:

- heat balance in EMAs is more difficult to ensure than in HSAs, in which the heat generated by the internal losses can be rejected through the hydraulic fluid and even through the natural heat exchange capability of the hydraulic tubes, returning to the reservoir. However, in EMAs the heat is produced in a closed volume, it has to be dissipated (or stored) at the actuator level, except in very specific applications where the actuator can be cooled by a dedicated fluid circuit.

- temperature effect on thermal balance is more severe. Conduction and switching losses in PDE, copper and iron losses in EM, and frictional losses in MPT are directly linked to the EMA operating temperature. The heat generated by all the above mentioned power losses is dissipated towards the local environment which may increase the EMA operating temperature and bring snowball effect within all the devices.

- lifespan and faults of EMA components are essentially due to the impact of temperature. Overheat may cause short-circuit or open-circuit in PDE, windings shorts and demagnetization of permanent magnet in EM, Dilation of MPT, etc. All of these are the potential faults that can lead to failure.

Therefore, thermal behavior of EMA needs to be taken into consideration in the actuator design and sizing process. However, at present, the current method for thermal behavior modeling and simulation of PbW actuator is using three dimensional (3D) finite element method (FEM) analysis. This method simulates the temperature distribution on the basis of the given detail design, e.g. EMA in [3] and EHA in [4]. Another common way for actuator thermal behavior analysis is to build an equivalent thermal network in the thermal field model, as presented in [5] and [6]. Unfortunately, for thermal behavior analysis, these simulation methods are very time-consuming and require the detailed geometries. In addition, it is not easy to analyze the thermal balance at the system-level, in the whole actuation system during a flight mission profile, including the variation of the environment temperature.

The present communication deals with the above reviews of the state of the art in thermal behavior modeling and simulation for aerospace PbW actuators. It considers the thermal environment conditions for the virtual prototype design of EMAs. Firstly, a typical cascade

control structure of EMA system is introduced to enable the flight mission profile to be followed. Then, the engineering needs are listed and best practices are proposed accordingly. A special attention is paid to the power loss and energy balance in the model and submodels of the whole EMA system. The model architecture and interfaces are defined in a structured manner with resort to the Bond-graph representation to comply with the different views of signal flows, power flows, heat flows and even fault flows. At last, a simplified thermal model and a more realistic one are compared to highlight the impact of model reduction on the accuracy of the simulated EMA temperature and the specific issues in considering the thermal effect in the simulation-based process of EMAs.

2 EMA System Descriptions

Currently, two types of linear EMAs are regarded for flight control or landing gears applications:

- geared type EMA: the mechanical power flows from the motor to the load through a gearbox then to a nut-screw mechanism;
- direct drive type EMA removes the gear reduction and offers a high potential for geometrical integration of the nut-screw reducer and the electric motor.

In this communication, a direct drive type EMA is considered, which is more suitable and competitive for aerospace applications because of its lower mass and more compact envelope. However, the thermal issue in this type of EMA is more serious and needs to be considered with more attention.

2.1 Typical Control Structure

As depicted in Fig. 1, the EMA is position servo controlled. It follows the pilot or autopilot demand (pursuit) and rejects the aerodynamic force disturbance (rejection). The EMA is controlled in a typical way using a cascade structure: current loop as the inner loop, velocity loop as the middle loop and position loop as the outer loop. Depending on the implementation, the upper control loops can be performed at actuator control system or flight control computer level. An overview of the control structure of the EMA is shown in Fig. 2.

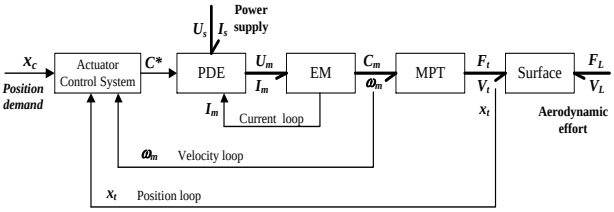

Fig. 2. Synoptic control structure of EMA

In Fig.2, typically an integrated resolver sensor provides the rotor position and velocity for motor field control while a linear variable displacement transducer (LVDT) provides the rod extension for surface position control.

2.2 Cross-linked Multi-domain Disciplines

At the system-level of EMA designing, modeling and simulation require multidisciplinary approach not only for preliminary power sizing and estimation of the mass and geometrical envelope, but also for the consideration of thermal behavior.

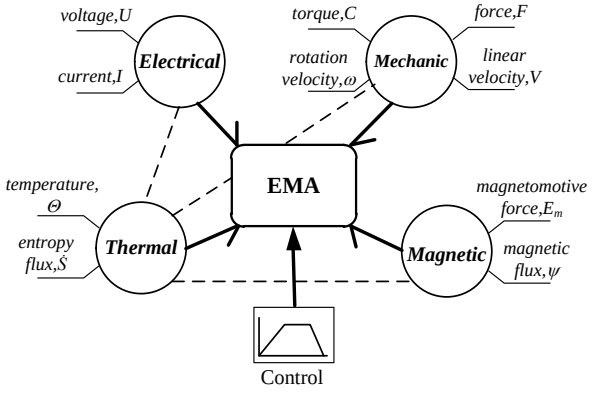

Fig. 3. Multi-domain Coupled in EMA

The cross-linked multi-domains are shown in Fig. 3. In this figure, power bonds by a half arrow in order to distinguish them from signal flows and power flows. Each bond transports power as the product of two power variables which involve some different physical quantities. The signal and power flows are explicitly differentiated. Power bonds propagate two power variables: voltage and current, torque and rotational velocity, force and translational velocity, etc. Full arrows indicate a signal flow

that carries only one type of information for control design (e.g: feedback or command signal).

2.3 Physical Effects

At the system-level of EMA virtual prototyping, it is found efficient to link the engineering needs and impacts to the physical effects to be modelled and simulated, the best model never being the most detailed one. Typically, the EMA model can be developed for simulation aided conceptual design (architectures and function), control design, thermal balance, mean and peak power drawn, etc., as shown in Tab.1.

In this manner, the model development is driven by needs and can be structured using an incremental approach [7]. The components' models can be made replaceable and balanced, whether each physical effect is considered or not, the complexity is progressively increased.

Table 1. Physical effects vs. engineering needs and impacts

Physical effects	Engineering Needs									Impacts			
	Functional (no parasitic effectl)	Power sizing	Thermal balance	Natural dynamics	Closed loop (stability/accuracy)	Consumed energy	Response to failure	Load propagation	Reliability	Numbers of parameters	Number of state variables	Duration of simulation time	Typical dynamics
A).Power Drive Electrics (PDE)													
1. Perfect power transformer	√	√	√	√	√	√	√	√	√			S	
2. Basic Model (linear/without power loss)				√	√					S	S	S	1ms
3. Advanced model (conduction, switching losses		√	√			√				M	M	M	
4. Full model (thermal, fault, etc)		√	√			√	√		√	L	L	L	100µs
B).Electric Motor (EM)													
1. Perfect power converter	√	√	√	√	√	√	√	√	√			S	
2. Basic Model (linear/without power loss)				√	√					S	S	S	
3. Advanced model (copper, iron, friction losses)		√	√	√	√	√		√		M	M	M	10ms
4. Full model (thermal, fault, etc)		√	√		√	√	√		√	L	L	M	
C).Mechanical Power Transmission (MPT)													
1. Perfect power transformer	√	√	√	√	√	√	√	√	√			S	
2. Basic Model (linear/ without power losses)				√	√					S	S	S	
3. Advanced model (friction loss, compliance, etc		√	√	√	√	√		√		M	M	M	10ms
4. Full model (thermal, fault, etc)		√	√		√	√	√		√	L	L	L	
√ = *Yes*										L	*Large*	L	*Long*
√ = *Possible (but depending on relative level)*										M	*Medium*	M	*Medium*
= *Not applicable (N/A)*										S	*Small*	S	*Short*

3 Heat Sources

The thermal behavior can be analyzed on the view of heat generation and power losses. This requires understanding the multidisciplinary coupling effects to model the impact of heat on temperature. So the virtual prototype to be developed shall realistically reproduce the physical effects and their coupling in electric, magnetic, thermal and mechanical domains. Making the models balanced (energetically and mechanically) is an important target for assessing coupled effects (e.g. EMA temperature rise due to losses in power electronics). For this reason, adopting the Bond-graph formalism [8] is particularly interesting for model structure definition. Meanwhile, all physical effects in EMAs can be considered.

3.1 EMA Model Decomposition

The virtual prototype of the EMA actuation system with thermal model is proposed to assess and pre-validate the thermal behavior with resort to a model-based approach. It is interesting to make EMA thermal model's structure consistent with the topology of the product but not the detailed geometry. Resorting to Bond-graph formalism, an decomposition example of a direct drive type linear EMA is illustrated in Fig.4 (a). EMA's model is made up of a combination of bodies (housing, shaft and rod) that are interconnected by bearings or joints (cylinder pair, hinge) and power transformation components (PDE, EM and NS). Fig 4 (b) shows the generic model element, which is standard, replaceable, and is mechanically and

thermally balanced: 2 degrees of freedom (2-DOF: Translation and Rotation) motions [9] with heat transfer. The implementation is proposed to enable these bi-directional couplings to be realistically simulated. In addition, the model can be re-used for other engineering needs or modeling purposes, such as energy consumption, natural and closed-loop performance and even response to failure, etc.

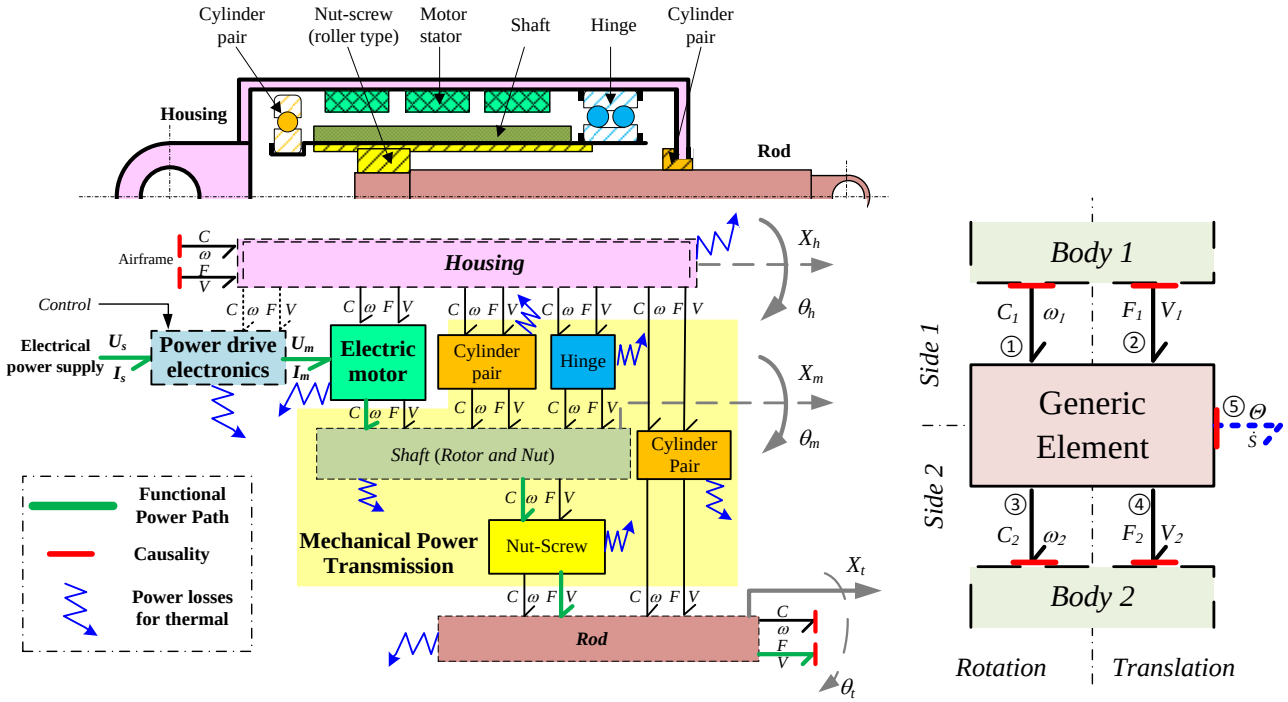

(a) Decomposition process of EMA (b) Causality of generic component

Fig. 4. Balancing Decomposition process of EMA

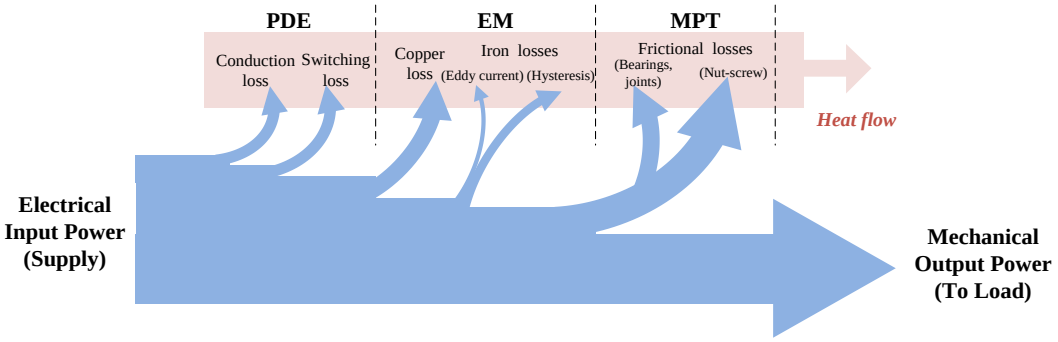

Fig. 5. Power flow transformed in EMA for driving a resistant load (steady state velocity)

3.2 Heat Flows of Energy Losses

Fig.5 shows an example of power flow when the EMA is driving a resistant load at constant speed, the heat power is generated by the different types of energy losses as from electric power (source supply) to mechanical power (output to the load).

According to the authors' former work presented in [10], the energy losses in EMAs can be divided into three main parts:

- *PDE losses*: conduction and switching losses
- *EM losses*: copper loss and iron losses (eddy current loss and hysteresis loss).
- *MPT losses*: nut-screw friction loss, bearings and joints losses.

Because of multidisciplinary domain coupled in EMA, the accurate equations to calculate these energy losses are difficult to present. Thus, the generic form of the equations

are summarized in Tab 2, in which the storage effects of power flows are also described.

For high level modeling, thermal behavior needs to be considered. The reason being in EMAs some physical aspects of power flow transformations are strongly dependent on instant operating temperature. The energy loss grows accordingly, causing a snowball effect. This produces a looped effect which cannot be neglected when the intention is to assess the thermal equilibrium of the EMA, like power losses and heat transfer.

Table 2. Summary of Power Flows Analysis in EMA

Power Flows				**Equations**	**Remarks**
Input	Electrical power form supply			$P_s = U_s I_s$	Electric
Losses	PDE	Conduction		$P_d = I_d^2 R_{on}$	Electric
		Switching		$P_{sw} = \left(E_{on} + E_{off}\right) f_{sw}$	Electric
	EM	Copper		$P_{co} = R_s I_s^2$	Electric
		Iron	eddy current	$P_{ed} = k_{ed} B_s \omega_m^2$	Electromagnetic
			hysteresis	$P_{hy} = k_{hy} B_s^2 \omega_m$	
	MPT	Frictional	joints	$P_{ft} = F_f V_r$	Electromagnetic
			nut-screw		
			bearings	$P_{fr} = C_f \omega_r$	Mechanical translation
Storage	PDE	Capacitors		$P_c = U_d C_{igbt} \frac{dU_d}{dt}$	Electrical
	EM	Winding inductance		$P_i = I_s L_s \frac{di_s}{dt}$	Electrical
		Cogging torque		$P_{cg} = C_{cg} \omega_r$	Mechanical rotation
	MPT	Rotational inertia		$P_j = J_m \omega_r \frac{d\omega_r}{dt}$	Mechanical translation
		Translational mass		$P_{ma} = M_{ns} v_r \frac{dv_r}{dt}$	Mechanical rotation
		Compliance		$P_k = k_e x_r \frac{dx_r}{dt}$	Mechanical translation
Output	Mechanical power to load			$P_o = F_t V_t$	Mechanical translation

3.3 Temperature Effects on Energy Losses

In normal operating conditions, the ambient temperature varies between -40 to 70°C. Temperature influences the energy losses, which may in turn affect the heat flow. The thermal modeling shall introduce the temperature effect of each device of EMA. The thermal behavior analysis is as follows. It is assumed that, Θ_1 is the actual operating temperature and Θ_0 is the reference temperature.

3.1.1 PDE Thermal Behavior

The on-state resistance (R_{on}) of transistor/diode is sensitive to the temperature, which results in forward voltage drop. So, the conduction loss of PDE can be assumed is first approximation to depend linearly on temperature:

$$\dot{Q}_{co} = I_d^2 R_{on}(1+\alpha_R(\Theta_1-\Theta_0)) \quad (1)$$

In addition, the switching loss in PDE has a weak dependency with temperature. However, it is poorly documented in the datasheets, and also can be assumed as:

$$\dot{Q}_{sw} = f_{sw}(E_{on}+E_{off})(1+\beta_R(\Theta_1-\Theta_0)) \quad (2)$$

3.1.2 EM Thermal Behavior

Motor winding resistance (R_s) is the main cause of heat generation within EM. As it is also temperature sensitive, the temperature coefficient (ε_R) is introduced to effect the change of copper conductivity:

$$\dot{Q}_{cu} = I_s^2 R_s(1+\varepsilon_R(\Theta_1-\Theta_0)) \quad (3)$$

The iron losses are usually calculated by referring to the information given by the lamination manufacturers for a rate flux density (B_s) and vs. motor velocity.

$$\dot{Q}_{ir} = (k_{ed}B_s^2\omega_m + k_{hy}B_s^{\gamma})\omega_m \quad (4)$$

The increase of motor temperature may decrease the performance of the magnets and affect the magnetic flux density. However, the temperature effects are poorly documented. In this paper, the iron losses are estimated by using the maximum flux density. Thus, the temperature influence on EMA magnet is ignored here.

3.1.3 MPT Thermal Behavior

It is well known that friction depends hugely on temperature. An in-depth analysis on modeling this effect at system-level has been presented in [11]. A simple way is to introduce a temperature dependent factor $\tilde{\mu}_{ft}(\Theta)$ to present the temperature effects on friction loss i.e, nut-screw transformation on translational domain by:

$$\dot{Q}_{ft} = F_{ft}V_r\tilde{\mu}_{ft}(\Theta) \quad (5)$$

Another consideration is the bearing losses in MPT which support rotation or translation functions. Generally, the power loss by bearing is the product of the frictional torque (C_{ft}) and the relative rotational speed (ω_r), given as:

$$\dot{Q}_{fr} = C_{fr}(\Theta)\omega_r \quad (6)$$

The temperature effects on the lubricant and viscosity can be considered in some advanced bearing loss model, like SKF [12].

4 Thermal Models of EMA

In this paper, the natural cooling capability of the EMA system is considered to simulate the worst case of the heat dissipation. The thermal model should represent the whole EMA components. In this framework, EMA is divided into three main parts with dissipative energy losses:

- PDE, involving conduction and switching losses,
- EM, (the stator, the rotor and the shaft) involving copper and iron losses,
- MPT, simplified to the nut-screw (roller type) and its bearings (cylinder pairs and hinges), involving frictional losses.

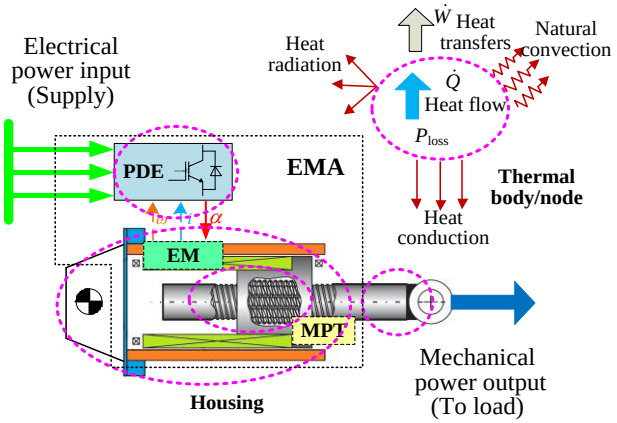

Fig. 6. Heat flow transfer in EMA

The heat generated by energy losses can be transferred via different ways, (conduction, convection and radiation) are between the multiple bodies/components of inner EMA or outer EMA, shown in Fig. 6. Thus, the architecting of the thermal model of heat transfer can be first considered in a simple way by assuming a single thermal capacitance or in an advanced way involving multiple thermal nodes. These two architectures have been simplified in following analysis to focus on the significant part for heat transfer and thermal exchanges.

4.1 Single Capacitance Model

For simple thermal modeling of EMA, shown in Fig. 7, a global body is considered as the housing. All of the energy losses heat the housing body which exchange to the ambient air.

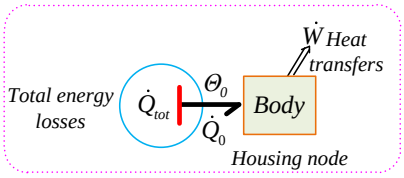

Fig. 7. Simple thermal model for heat transfers

The corresponding causal Bond-graph thermal model is shown in Fig. 8, introducing a single heat capacity of $C_{housing}$. The heat exchange with ambiance is presented by R_{ex}.

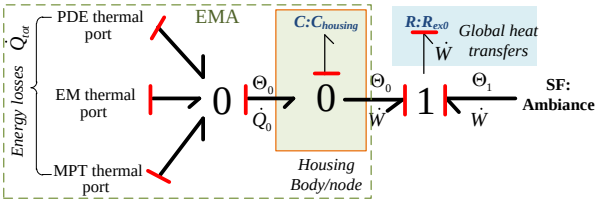

Fig. 8. Causal Bond-graph thermal model of EMA (simple)

The basic equation of the thermal balance applied on the housing body, is described as:

$$\dot{Q}_{tot} - \dot{W} = C_{housing} \frac{d\Theta_0}{dt} \qquad (7)$$

4.2 Advanced Model

According to the decomposition structure for more realistic topology of EMA in Fig. 4 (a), the heat generated by the energy loss of each component is transferred not only to one thermal body or node but to other different bodies. In this paper, three different bodies are considered: housing, shaft and rod. The thermal phenomena modelled are:

- The heat generated by energy losses of PDE can be transferred to ambiance and to EMA housing,
- The heat in EM can be transferred to the housing (stator) and to the shaft (rotor),
- In MPT, the heat produced in nut-screw can be transferred to the shaft (nut) and to the rod (screw),
- Also in MPT, concerning to other components, for example, the heat in hinge can be transferred to housing and shaft. The heat in cylinder pair (of rod) can be transferred to the housing and to the rod.

Thus, the generic advanced thermal model for heat transfers can be presented in Fig.9. The heat generated by the energy loss may be transported via two different thermal bodies, in which different heat capacity and heat transfer rates can be considered.

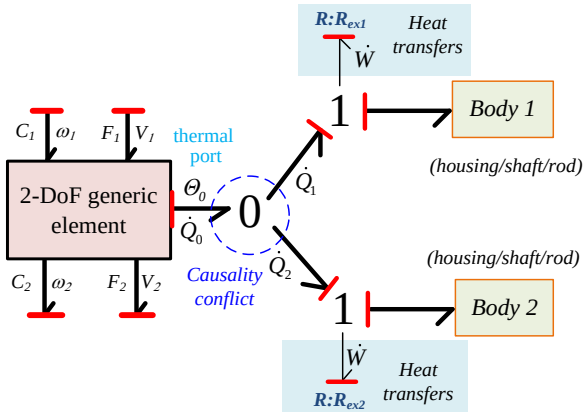

Fig. 9. Generic advanced thermal model

Remarks: Thanks to the Bond-Graph formalism, a causality conflict is pointed up in this generic advanced thermal model. Therefore, this paper proposes three different ways of causality conflict for simulation implementation:

(1). implementation in today's non-causal simulation software, such as Modelica, this generic advanced thermal model can be directly implemented.

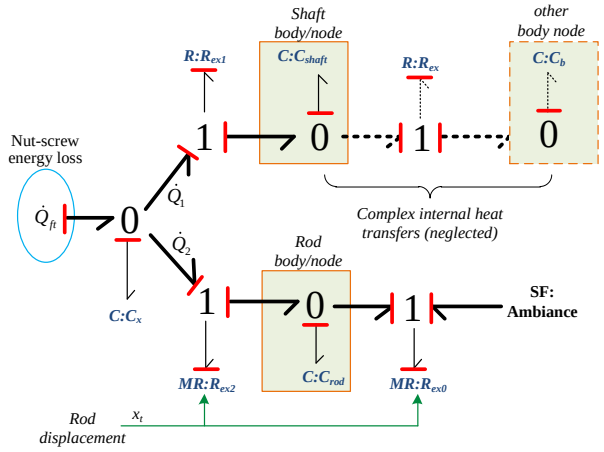

Fig. 10. Example of the causal Bond-graph thermal model of nut-screw (advanced)

(2). For causal simulation, a specific heat capacity (C_x) can introduced for each body to eliminate the causality conflict. Thus, the proposed causal Bond-Graph thermal model can be given in Fig. 10, the nut-screw generic model.

In nut-screw MPT components, the heat generated of friction loss can be transferred to the shaft (nut) body and to the rod (screw) body. As shown in Fig. 10, thus, two heat capacities C_{shaft} and C_{rod} are introduced, respectively. If considered the internal heat transfer ways, the heat of the shaft body can be transferred to or exchange with other bodies, represented by (R_{ex}), such as to housing body. Meanwhile, as the rod is in contact with ambient air, the heat can be transferred to the ambiance. However, because of the EMA servo demand and the displacement of the rod (X_t), the contact area is varing and it will modulate the heat transfer parameters (R_{ex2} and R_{ex0}), R element to MR element in Bond-graph. This solution requires additional parameters and increased the simulation time.

(3). As an alternative to the second solution a "flow contribution factor" $k_Q \in [0,1]$ is proposed, and it is assumed that the heat power flow is shared between each bodies. Each heat flow to the thermal body then depends on the EMA generic component energy loss as a function of the k_Q factor, as follows:

$$\dot{Q}_1 = k_Q \dot{Q}_0 \qquad (8)$$

$$\dot{Q}_2 = (1 - k_Q)\dot{Q}_0 \qquad (9)$$

4.3 Heat Transfer and Exchange

In the proposed single capacitance or advanced thermal models, the heat transfer (R_{ex}) is achieved by conduction, convection and radiation. The heat transfer coefficients [13] are always dependent on a lot of variables, such as: solid geometry, contact area, material, flow conditions, air characteristic properties, etc. They are difficult to predict with accuracy. However, the inner mechanism structure of EMA is very complex. Therefore, it is very difficult to introduce some complex geometry parameters or variables, which are nonlinear, especially when EMA is working in the specific operating conditions.

Beside the thermal models architecting, there is still a huge effort to be placed towards parameters identification process and knowledge capitalization.

5 Conclusions

Bond-graph modeling has been used to support the development of the EMA thermal model architectures with a system-view. It was dedicated to the adverse link, with detailed analysis and modeling of the impact of the temperature on EMA behavior. Firstly, a single capacitance thermal model has been proposed to consider a global thermal body/node for EMA functional energy balance. Then, detailed physical effects according to the proposed EMA decomposition process have been considered in an advanced thermal model. Three different thermal body/node were selected that keep EMA both mechanically and thermal balanced. The proposed models are incremental and generic ensuring continuity between the engineering activities, knowledge capitalization and multi-physical nature of actuation. In addition, both the simple and advanced models are causal. The models are ready to be extended for next step thermal transfers simulation and for sizing and designing the heat-sink for EMA actuation.

Notations

B_s	Magnetic saturation flux density	[T]
C^*, C_{cg}, C_f, C_m	Command, cogging, frictional, motor output torque	[Nm]
C_{igbt}	IGBT capacitance	[F]
C_b, $C_{housing}$, C_{rod}, C_{shaft}, C_x	Specific heat capacity of body, housing, rod, shaft and generic component	[$J/kg/K$]
E_{on}, E_{off} , E_{sw}	Switch turn-on, turn off , total switching losses	[J]
F_{ft}	Friction force	[N]
F_t, F_L	EMA rod and aerodynamic force	[N]
f_{sw}	Switch frequency	[Hz]
I_s, I_m, I_d	Supplied DC, motor and motor average current	[A]
J_m	Rotor inertia	[kgm^2]
k_e	Mechanical transmission stiffness	[N/m]
k_{ed}, k_{hy}	Eddy current and hysteresis constant	[-]

k_Q	Flow contribution factor	[-]
L_s	Motor winding inductance	[H]
M_{ns}	Nut-screw equivalent mass	[kg]
P_{co},P_d, P_{sw}	Copper, conduction, switching power losses	[W]
P_{ft}, P_{fr}	Translational , rotational friction losses	[W]
P_c, P_{cg}, P_i, P_j, P_k, P_{ma}	IGBT capacitor, cogging torque, inertial, mass, compliance storage power	[W]
P_{ed}, P_{hy}	Eddy current and hysteresis losses	[W]
P_o	EMA output mechanical power	[W]
$\dot{Q}_{co}$ $\dot{Q}_{sw}$ $\dot{Q}_{cu}$ $\dot{Q}_{ir}$ $\dot{Q}_{ft}$ $\dot{Q}_{fr}$	Heat flow of conduction, switching, copper, iron, translational friction, rotational friction losses	[W]
$\dot{Q}_0$ $\dot{Q}_1$ $\dot{Q}_2$	Generic EMA component, body 1 and body 2 heat flow	[W]
$\dot{Q}_{tot}$	EMA total heat flow	[W]
R_{on}, R_s	Transistor/diode on-state, motor winding resistance	[Ω]
U_d, U_s, U_m	IGBT supplied, DC supplied and motor armature voltage	[V]
V_t, V_L	EMA rod and aerodynamic load velocity	[m/s]
v_r	Relative velocity in mechanical transmission	[m/s]
$\dot{W}$	Heat transfers flow	[W]
x_c, x_t, x_r	EMA position command, rod, relative displacement	[m]
Θ_1, Θ_0	Actual operating and reference temperature	[$°C$]
α_R	Temperature dependency of electrical resistance,	[-]
β_R	Temperature dependency of switching loss	[-]
ε_R	Temperature dependency of magnet materials	[-]
$\tilde{\mu}_{ft}$	Temperature sensitivity friction factor	[-]
ω_m, ω_r	Motor, mechanical transmission relative velocity	[rad/s]

Copyright Statement

References

[1] Roboam X, Sareni B and Andrade A D. More electricity in the air: Toward optimized electrical networks embedded in more-electrical aircraft. *IEEE Industrial Electronics Magazine*, Vol. 6, No. 4, pp 6-17, 2012.

[2] Derrien J-C, Tieys P, Senegas D, et al. EMA Aileron COVADIS Development. *SAE Technical Paper*, 2011.

[3] Pasies-Rubert O, Mur C, Garay M, et al. Benefits of multiphysics models integration through cosimulation case study: heat monitoring on a Primary Flight Control EMA. *International Conference on Recent Advances in Aerospace Actuation Systems and Components (R3ASC)*, Toulouse, pp 144-149, 2014.

[4] Takebayashi W and Hara Y. Thermal design tool for EHA.*Proc of International Conference on Recent Advances in Aerospace Actuation Systems and Components (R3ASC)*, Toulouse, pp 15-20, 2004.

[5] Björn J, Johan A and Petter K. Thermal modelling of an electro-hydrostatic actuation system. *International Conference on Recent Advances in Aerospace Actuation Systems and Components*, Toulouse, pp 13-15, 2001.

[6] Li K, Lv Z, Lu K, et al. Thermal-hydraulic Modeling and Simulation of the Hydraulic System based on the Electro-hydrostatic Actuator. *Procedia Engineering*, Vol. 80, No. 0, pp 272-281, 2014.

[7] Fu J, Maré J-C, Fu Y, et al. Incremental modelling and simulation of power drive electronics and motor for flight control electromechanical actuators application. *IEEE International Conference on Mechatronics and Automation (ICMA)*, Beijing, pp 1319-1325, 2015.

[8] Borutzky W. *Bond Graph Methodology: Development and Analysis of Multidisciplinary Dynamic System Models*New York: Springer, 2010.

[9] Maré J-C. 2-D lumped paramaters modelling of EMAs for advanced virtual prototyping. *International Conference on Recent Advances in Aerospace Actuation Systems and Components (R3ASC)*, Toulouse, pp 122-127, 2012.

[10] Fu J, Mare J-C and Fu Y. Modelling and simulation of flight control electromechanical actuators with special focus on model architecting, multidisciplinary effects and power flows. *Chinese Journal of Aeronautics*, 2016.

[11] Maré J-C. Friction modelling and simulation at system level: Considerations to load and temperature effects. *Proceedings of the Institution of Mechanical Engineers, Part I: Journal of Systems and Control Engineering*, Vol. 229, No. 1, pp 27-48, 2015.

[12] SKF. SKF General Catalogue. ed, 2006.

[13] Bergman T L, Incropera F P and Lavine A S. *Fundamentals of heat and mass transfer*. 7th edition: John Wiley & Sons, 2011.